

A LINEAR POWER AMPLIFIER WITH CURRENT INJECTION (LACI) FOR MAGNETIC BEARINGS

Johann Wassermann

Helmut Springer

Department of Mechanical Engineering
Technical University of Vienna, Austria

ABSTRACT

Efficiency and power consumption of an active magnetic bearing are primarily determined by the system that is used for power amplification. In this paper a new concept is presented that combines the advantages of a common analog power amplifier with those of a switching amplifier. The advantage of the new concept compared with the properties of a common switching amplifier is shown both by numeric simulation results and experimental measurements.

INTRODUCTION

The principle of an active magnetic bearing is based upon several current or voltage controlled electromagnets (actuators) by which attractive magnetic air gap forces are exerted to the structure to be supported, for example, a rotor, [1]. The power amplifier has to supply the coil current to the solenoid necessary to generate the required magnetic field strength. It is highly desired to transform the controller output signals without any significant distortion into the required magnetic field forces within a sufficiently high frequency range. In general, a transient distortion is primarily caused by the inductive reactance of the solenoid. A highly undistorted transformation of the controller signals under dynamic conditions requires considerable effort in the amplifier design, [2].

There are two design limits between which a power amplifier has to operate. First, for the static operation, a pure ohmic resistance in the coils of the actuator is present, and the system is controlled by a quite low voltage. This voltage is determined by the required maximum amount of DC within the coil and the residual voltage of the analog amplifier. Second, when operating an active magnetic bearing under highly dynamical

conditions (i.e. control of high-frequency disturbances that require high actuator force slew-rates) the frequency proportional impedance of the actuator becomes effective. In order to meet the required current slew rates in the actuator coils, in general, a supply voltage of more than 100 V is necessary. For example, for a coil inductivity of 10 mH and a required current slew rate of 15 A/ms a voltage of 150 V is needed, see [3]. Since analog amplifiers cause substantial losses at static or quasi-static operating conditions the performance requirements for the limit states lead to the application of a switching concept, [3, 4, 5].

In switching amplifiers, high voltage and high current is present in the control devices (power-MOSFETs) only during the switching operations. The comparatively small switching losses are proportional to the supply voltage, and proportional to the switching-transition period and -frequency. There is practically no current flow for the power-MOSFET OFF-state conditions, and the power loss for the ON-state conditions is proportional to the ohmic resistance of the switching element and the square of the current.

Beside the advantage of small power losses of a switching amplifier there is also a big disadvantage. Because of the periodic switching process the control current is superimposed with a considerable number of higher harmonics, for example, the symmetric sawtooth control signal of a bang-bang switching amplifier or the variable sawtooth form of a PWM-controlled switching amplifier. The higher harmonics of the control current both cause undesirable forces exerted to the structure and generate eddy current and hysteresis losses within the material of the structure that may lead to thermal problems of the magnetic bearing.

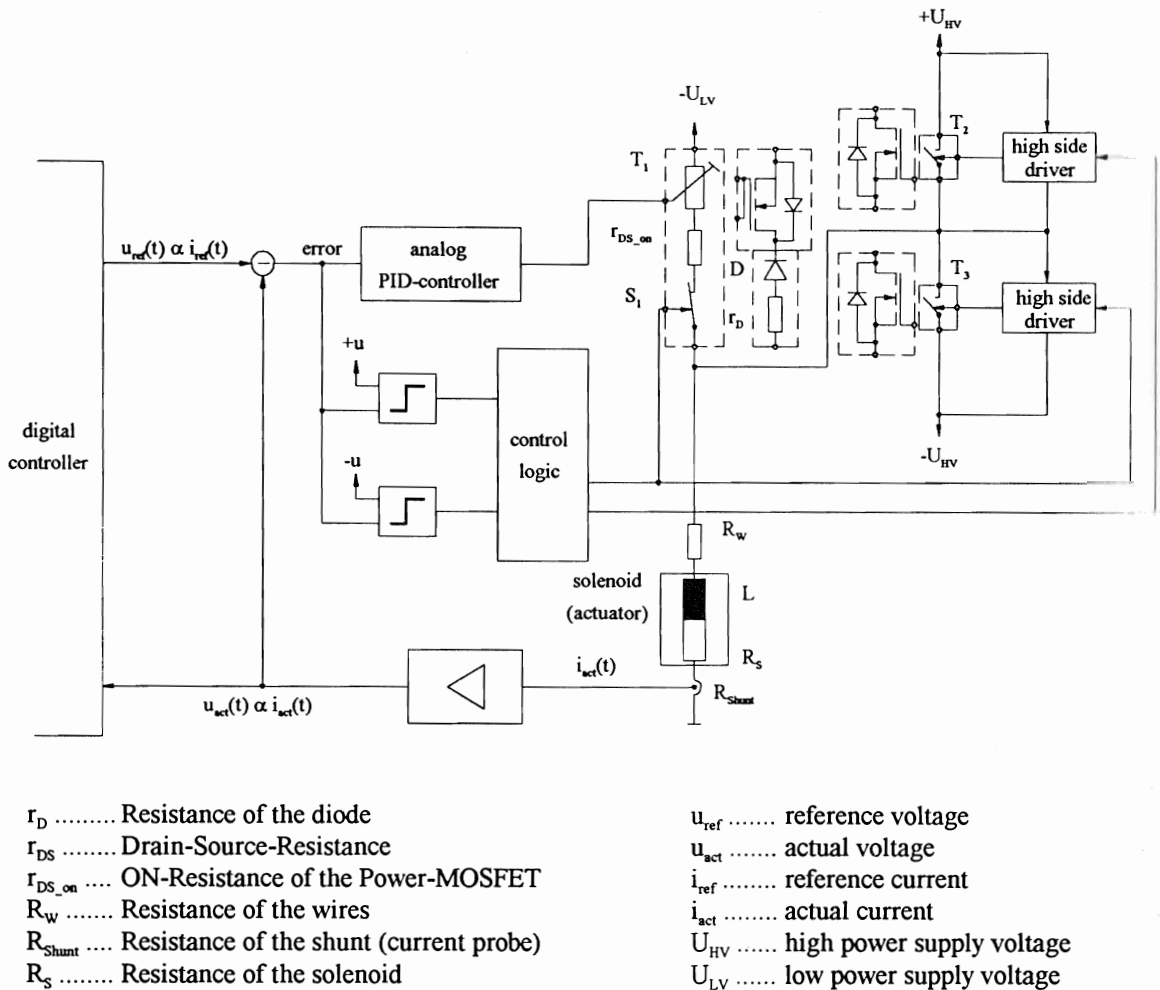


FIGURE 1: Block diagram of the LACI-concept

DESIGN OF THE POWER AMPLIFIER "LACI"

The new developed concept of an analog amplifier with current injection (Linear Amplifier with Current Injection = LACI) makes it possible to eliminate the above mentioned disadvantages of a common switching amplifier and retain the advantage of relatively small power losses. The principle schematic of LACI is shown in Fig. 1. It is based upon an appropriate circuit assembly of an analog and a switching amplifier, a cascade current controller, and a control logic unit. Depending on the operating conditions (either static, quasi-static, or highly dynamic) the logic unit automatically activates the corresponding part of LACI (either analog or switching amplifier). In Fig. 1 the analog amplifier T_1 is shown as a variable resistance, while the switching amplifier is represented by the switches T_2 and T_3 . When the switching amplifier is activated the switch S_1 disconnects the analog amplifier.

In the practical design solely N-channel power-MOSFETs (N-MOSFETs) are used for the control devices. In comparison to P-MOSFETs, N-MOSFETs show lower ON-resistance, handle higher blocking

voltage and enable higher switching current. Negative voltage peaks are blocked by D to prevent short circuiting of the low-voltage supply via the integrated recovery diode of T_1 . During normal operation the recovery diode of T_2 and T_3 are in OFF-state. The polarity of the recovery diodes is changed if a voltage of $\pm U_{HV}$ is exceeded, causing energy feedback to the corresponding high voltage power supply. In this way the high-peak voltages on the inductive load due to the switched current are suppressed very effectively.

The actual operating state of the amplifier is recognized by comparing the actual voltage $u_{act}(t)$ (proportional to the actual coil-current $i_{act}(t)$) with a reference voltage $u_{ref}(t)$. The actual current $i_{act}(t)$ is transformed into a proportional voltage signal $u_{act}(t)$ by using a floating current-voltage converter, for example, a Honeywell CSNE152. The reference control circuit supplies a voltage $u_{ref}(t)$ proportional to the desired reference coil-current of the actuator. If the error $e = \text{abs}[u_{ref}(t) - u_{act}(t)]$ is below a given limit value, then steady-state or quasi-steady-state operating conditions are recognized. Then

the analog part T_1 in Fig. 1 controls the current, and the switching amplifier (T_2, T_3) is inactive.

If the error exceeds a given limit value, then (depending on the polarity) an antiphase current is injected by the switching amplifier (T_2 or T_3 , respectively) until the control deviation lies again within the operating range of the analog amplifier. At this moment the switching amplifier is deactivated.

T_2 and T_3 are controlled through 500 V high-side drivers resulting in low response time and low control power demand. In addition, the operating point of the N-MOSFETs trigger signal is stabilized regardless of deviations of the supply voltage U_{HV} , and therefore no stabilizing of the voltage U_{HV} is necessary.

In order to avoid high-frequency switching processes when passing over the error limit the characteristic of the control logic unit contains a hysteresis. The supply voltage of the switching amplifier ranges between ± 150 V (or even higher) which guarantees a sufficiently high slew rate of the required current. A basic amplifier concept is mentioned in [6], where two separated voltage supplies (similar to the present concept) and two Darlington-transistor pairs in parallel were used. However, there is no detailed description presented about the design and the operating performance.

The layout of the low-voltage supply is given through the maximum current demand at static or quasi-static operation. The "static-state" supply voltage U_{LV} results from this maximum current requirement and the total ohmic resistance along the current path ($R_{ges} = r_{DS, on, T1} + r_D + R_S + R_{Shunt} + R_W$, Fig. 1). For example, if a compensation of harmonic forces (e.g. unbalance of a rotor) in a given system requires a current of 0.5 A, then up to a rotor speed of 10 000 rpm a ripple free control is achieved at about $U_{LV} = 12$ V, $L = 10$ mH without applying the current injection capability, resulting in much lower phase shift than achievable with current industrial amplifiers for magnetic bearings.

The maximum power loss within the analog amplifier results for a symmetric dividing of the voltage between the transistor T_1 and the solenoid. For example, a coil resistance of $R_S = 1 \Omega$ under a supply voltage of 10 V yields a maximum power loss of 25 W within the transistor.

The overall power losses of the switching amplifier consist of the conduction losses and the switching losses as mentioned above. The conduction losses can be kept at a low level if the transistor ON-resistance is as small as possible. For example, for $R_{DS, on} = 0.06 \Omega$ and $i = 8$ A the loss is about 4 W. The switching losses of the LACI-concept are significantly lower than those of a common switching amplifier since no steady state high frequency switching processes are required, and the amplifier is switched on and off only with the frequency of the occurrence of a large disturbance. The cascade control concept is a PID-controller in analog design. The

PID-controller is optimized together with the analog amplifier and guarantees an optimum performance of the overall cascade control circuit.

SIMULATION RESULTS

The numerical simulation was carried out by the software package MATLAB along with the graphical user interface SIMULINK. Both the new amplifier concept LACI and a model of a common switching amplifier were combined with a two-axes linear magnetic bearing model in order to study the time responses of the control current and the bearing forces. Two different amounts of unbalance were applied as an external excitation for both models.

Fig. 2 shows a block diagram of the LACI simulation model. The reference current supplied by the controller is compared with the actual current and limited within the modulation range of 0 A to 10 A (I_{range}). The output error is amplified by a simple P-controller by a factor of 1000. The solenoid of the bearing actuator ($R_S = 0.8 \Omega$, $L = 20$ mH) is analog controlled by the output signal within the low-voltage range of $0 \leq U_{LV} \leq 10$ V. As long as the deviation does not exceed the adjusted hysteresis values (Hyst1, Hyst2) no current injection is applied by the high-voltage device $\pm HV$, and the OFF-switch remains in the GND-position. If the output error exceeds the adjusted hysteresis values, then the solenoid is supplied with the high voltage through the summation block SUM2 by HV- and OFF-switches.

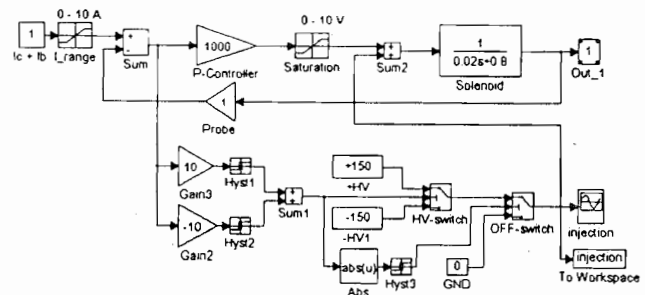


FIGURE 2: Block diagram of the LACI simulation model

In Fig. 3 the time responses of the control current in the solenoid and the corresponding control voltage are shown for a fairly small unbalance eccentricity of the rotor mass ($e = 2 \mu\text{m}$) at 4000 rpm. The right hand side of the figure corresponds to the common switching amplifier, the left one to the LACI-concept that still operates in the analog state, i.e. $U_{HV} = 0$. It is obvious that in the latter case no switching losses, and no high frequency induced hysteresis- and eddy current losses are generated by the LACI-system. For a comparatively high eccentricity ($e = 200 \mu\text{m}$) at the same speed the corresponding simulation results are presented in Fig. 4. It

can be seen that only for high current slew rates the switching capability of LACI is activated. Even from the current time responses it is recognized that the common switching amplifier generates a lot more higher harmonics than the LACI-system. In magnetic bearings therefore, the LACI-system causes much less eddy current losses compared with a switching amplifier.

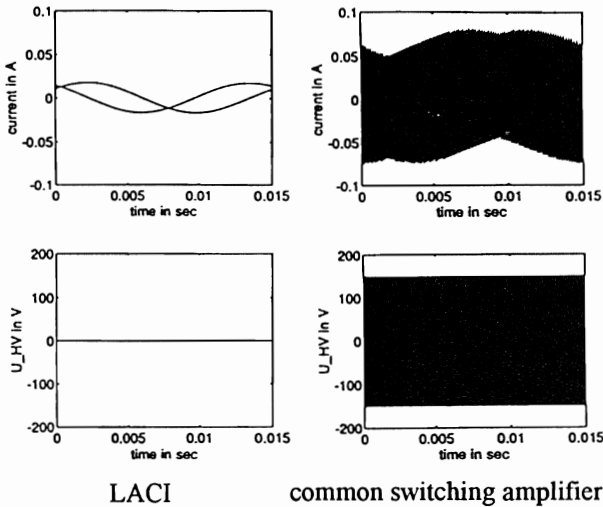


FIGURE 3: Time response of the control current with small unbalance eccentricity ($e = 2 \mu\text{m}$, rotor mass = 14 kg, $n = 4000 \text{ rpm}$)

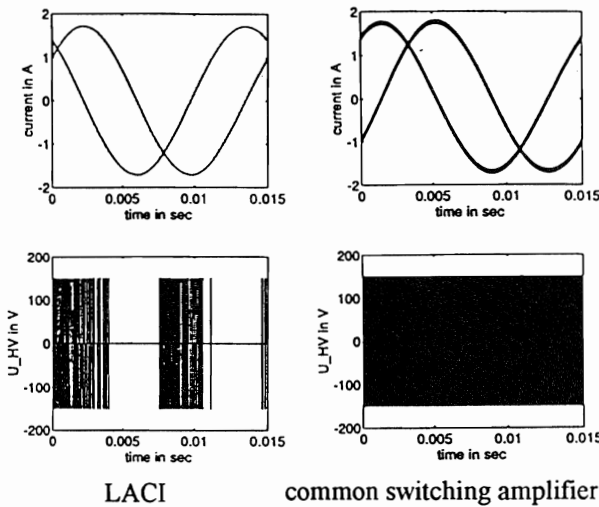


FIGURE 4: Time response of the control current with an unbalance eccentricity of $e = 200 \mu\text{m}$

MEASUREMENT RESULTS

In order to experimentally verify the above numerical simulation results measurements were carried out on a real electromagnetic actuator (load capacity $F = 1 \text{ kN}$, $R_s = 0.56 \Omega$, $L = 12 \text{ to } 30 \text{ mH}$). The comparison was made between an industrial switching amplifier as a reference and the new LACI-concept. The results are shown in Fig. 5 to 8. The characteristics of figure part

(a) corresponds to the LACI-device, figure part (b) corresponds to the switching amplifier, respectively. Fig. 5 and 6 show the time response characteristics of both amplifiers at 100 Hz and 1 kHz, respectively, for a sinusoidal reference current signal. For both frequencies the LACI-device shows much less signal distortions concerning amplitude reduction and phase shift. In particular, for the 1 kHz frequency the reference amplifier (Fig. 6b) generates a significant decrease of the current amplitude and a dramatic phase shift. In addition, Fig. 6a shows the control signal for the current injection and the current deviation $e = i_{ref} - i_{act}$, see Fig. 1.

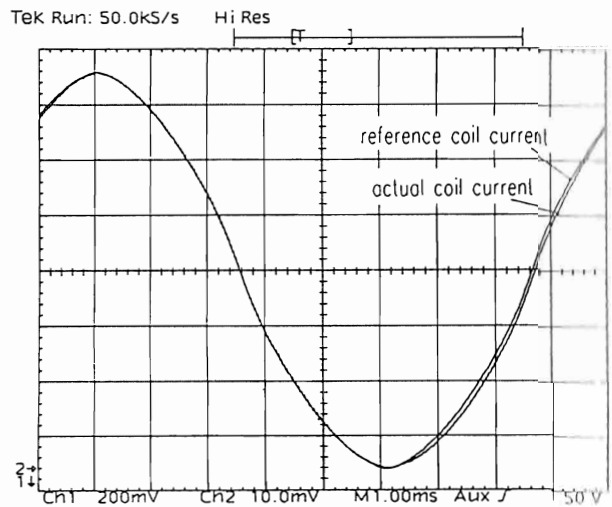


FIGURE 5a: Time response of the LACI for sinusoidal reference current signal ($f = 100 \text{ Hz}$, $I_b = 0.72 \text{ A}$, $I_c = 1.4 \text{ A}_{pp}$)

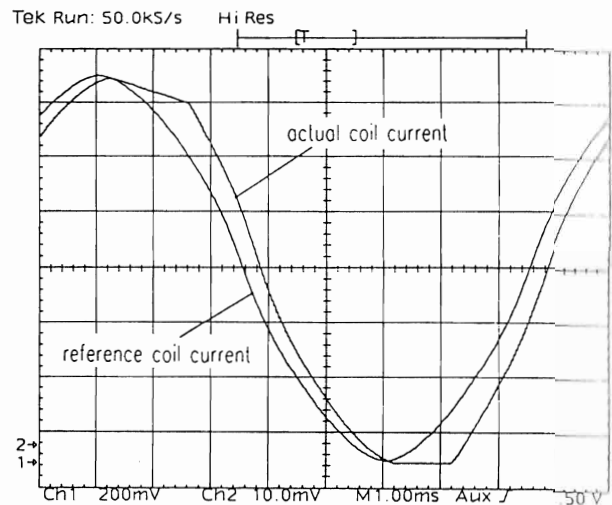


FIGURE 5b: Comparative time response of the industrial switching amplifier

A significant decrease in amplitude of the reference switching amplifier with increasing frequency can be seen also from the frequency response transfer function

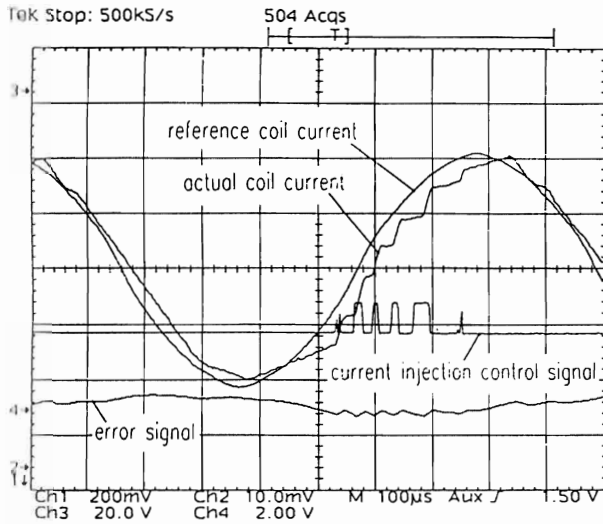


FIGURE 6a: Time response of the LACI for sinusoidal reference current signal ($f = 1 \text{ kHz}$, $I_b = 0.66 \text{ A}$, $I_c = 0.84 \text{ A}_{pp}$)

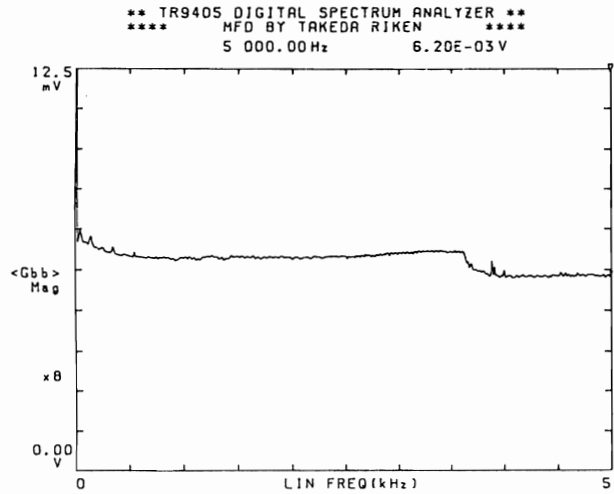


FIGURE 7a: Frequency response transfer function of the LACI ($I_b = 1 \text{ A}$, $I_c = 0.4 \text{ A}_{pp}$, sinusoidal sweep)

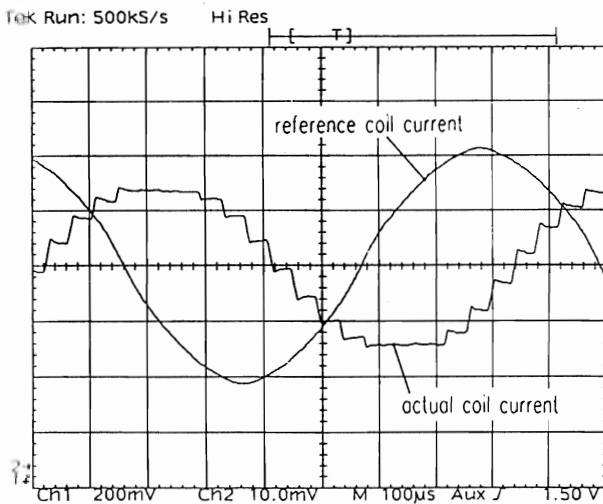


FIGURE 6b: Comparative time response of the industrial switching amplifier

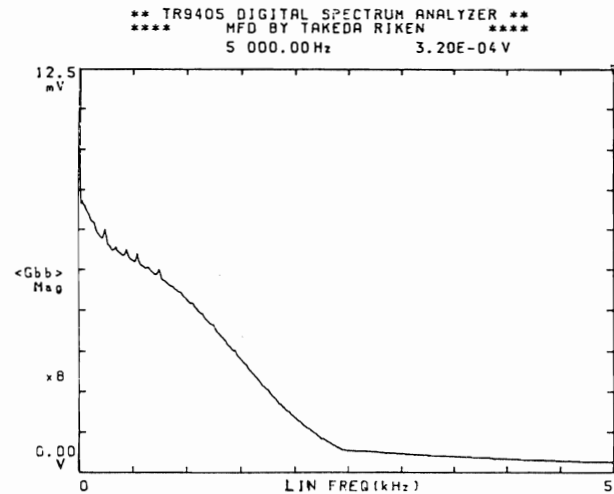


FIGURE 7b: Comparative frequency response transfer function of the industrial switching amplifier

in Fig. 7b, ($I_b = 1 \text{ A}$, $I_c = \pm 200 \text{ mA}$, sinusoidal sweep). Up to 3.5 kHz the LACI-device shows almost a constant frequency response characteristic which is obviously not the case for the reference amplifier.

The measured step response characteristics are presented in Fig. 8. For a reference control current step of $I_c = 3 \text{ A}$ ($I_b = 4 \text{ A}$, $U_{HV} = 100 \text{ V}$) the common switching amplifier displays a delay time of about $100 \mu\text{s}$ and a rise time of $300 \mu\text{s}$, see Fig. 8b. For the same high-voltage supply of $U_{HV} = 100 \text{ V}$ the LACI-device displays the same rise time (climbing period), however

without any significant delay time, see Fig. 8a. In this figure the control signal for the current injection is additionally documented. It shows a constant amount of current injection during the climbing period followed by a few and short injection intervals after the ramp. These short current injections may be suppressed easily by the control logic unit (see Fig. 1) if a smoother transition between the ramp and the static level is acceptable.

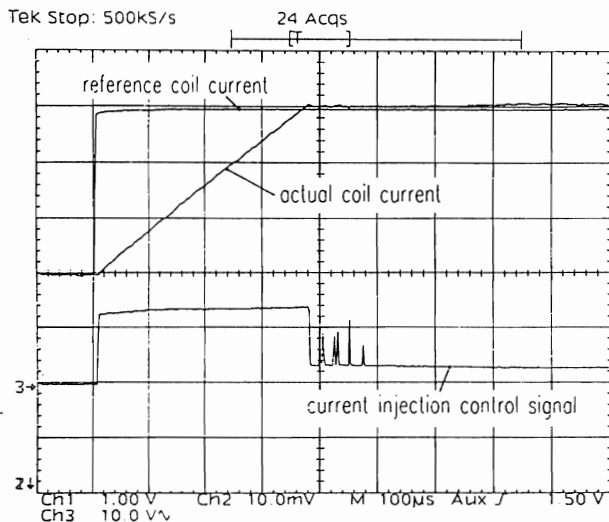


FIGURE 8a: Step response characteristics of the LACI ($I_b = 4$ A, $I_c = 3$ A, $U_{HV} = 100$ V)

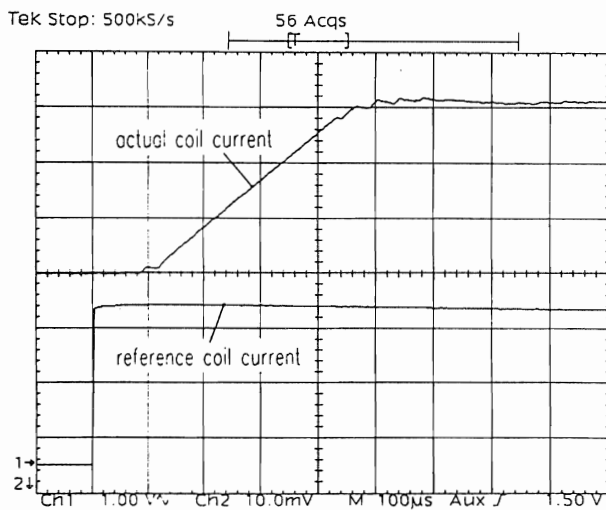


FIGURE 8b: Comparative step response characteristic of the industrial switching amplifier

CONCLUSION

Comparative simulation results between models of a common industrial switching amplifier and a new amplifier design LACI for magnetic bearings show a much better performance of the LACI-concept, in particular under static or quasi-static operating conditions. The new amplifier generates much less high frequency components in the coil current, and therefore thermal problems due to eddy current in the rotor material can be

suppressed or are at least highly reduced. The simulation results were accurately verified by measurements carried out on a real magnetic bearing actuator. In the high frequency range the new amplifier concept displays almost no amplitude and phase distortion and the step response function shows particularly no time delay except the limited current slew rate due to the inductive resistance of the bearing solenoid. By a sophisticated circuit design the hardware effort for the new amplifier system can be kept on a very reasonable low level.

REFERENCES

1. Schweitzer, G., A. Traxler, H. Bleuler, Magnetlager, Springer-Verlag, 1993.
2. Maslen, E. H., P. Hermann, M. Scott, R. R. Humphris, Practical Limits to the Performance of Magnetic Bearings: Peak Force, Slew Rate, and Displacement Sensitivity, *Journal of Tribology*, April 1989, Vol. 111, pp. 331 - 336.
3. Bardas, T., T. Harris, C. Oleksuk, G. Eisenbart, J. Geerlings, Problems, Solutions and Applications in the Development of a Wide Band Power Amplifier for Magnetic Bearings, 2nd International Symposium on Magnetic Bearing, July 12-14, 1990, Tokyo, Japan, pp. 219 - 227.
4. Keith, F. J., E. H. Maslen, R. R. Humphris, R. D. Williams, Switching Amplifier Design for Magnetic Bearings, 2nd International Symposium on Magnetic Bearing, July 12-14, 1990, Tokyo, Japan, pp. 211-218.
5. Kanemitsu, Y., M. Ohsawa, K. Watanabe, Active control of a flexible rotor by magnetic bearing - effect of power amplifier on unbalance response of rotor, *IMEchE-6*, 1992, pp. 111 - 114.
6. Delprete C., G. Genta, S. Carabelli, Design, Construction and Testing of a Five Active Axes Magnetic Bearing System, 2nd International Symposium on Magnetic Suspension Technology, 1993, Vol. 1, pp. 5a-21 - 5a-35.

ACKNOWLEDGMENTS

The authors thank the Austrian Science Foundation (FWF) for supporting this project. The Institute of Machine Dynamics and Measurement at TU-Vienna is gratefully acknowledged for laboratory, instrumentation and computer supply. Further thanks go to our colleague, Dipl.-Ing. O. Lang for his helpful support in simulation.